

Weak Measurement of Superconducting Qubit Reconciles Incompatible Operators

Jonathan T. Monroe,^{1,*} Nicole Yunger Halpern,^{2,3,4,5,†} Taeho Lee,¹ and Kater W. Murch^{1,‡}

¹*Department of Physics, Washington University, St. Louis, MO 63130, USA*

²*ITAMP, Harvard-Smithsonian Center for Astrophysics, Cambridge, MA 02138, USA*

³*Department of Physics, Harvard University, Cambridge, MA 02138, USA*

⁴*Research Laboratory of Electronics, Massachusetts Institute of Technology, Cambridge, MA 02139, USA*

⁵*Institute for Quantum Information and Matter,*

California Institute of Technology, Pasadena, CA 91125, USA

(Dated: May 27, 2022)

Traditional uncertainty relations dictate a minimal amount of noise in incompatible projective quantum measurements. However, not all measurements are projective. Weak measurements are minimally invasive methods for obtaining partial state information without projection. Recently, weak measurements were shown to obey an uncertainty relation cast in terms of entropies. We experimentally test this entropic uncertainty relation with strong and weak measurements of a superconducting transmon qubit. A weak measurement, we find, can reconcile two strong measurements' incompatibility, via backaction on the state. Mathematically, a weak value—a preselected and postselected expectation value—lowers the uncertainty bound. Hence we provide experimental support for the physical interpretation of the weak value as a determinant of a weak measurement's ability to reconcile incompatible operations.

Quantum measurements suffer from noise that limits precision metrology [1, 2], amplification [3, 4], and measurement-based feedback. The minimal amount of noise achievable is lower-bounded in uncertainty relations. They highlight how quantum noise arises from disagreement between, or incompatibility of, quantum operations. Robertson proved [5] the most familiar uncertainty relation: the measurement statistics of two observables, A and B , must have sufficiently large standard deviations, ΔA and ΔB , to obey

$$\Delta A \Delta B \geq \frac{1}{2} |\langle [A, B] \rangle|. \quad (1)$$

Operator pairs with nonzero uncertainty bounds are said to disagree, or to be incompatible. Uncertainty relations quantify the incompatibility.

Inequality (1) suffers from shortcomings [6]. For example, the right-hand side (RHS) depends on a state, through an expectation value. Varying the state appears to vary the disagreement between A and B . But the amount of disagreement should depend only on the operators. This objection and others led to the development of *entropic uncertainty relations* in quantum information theory [7]. The variances in Ineq. (1) give way to entropies, which quantify the optimal efficiencies with which information-processing tasks can be performed [8].

An exemplary entropic uncertainty relation was proved in [9]. Consider preparing a state ρ and measuring the observable A . Let p_a denote the probability of obtaining the eigenvalue a . The probability distribution $\{p_a\}$ has a Shannon entropy $H(A)_\rho := -\sum_a p_a \log_2 p_a$ equal to the detector's von Neumann entropy. If $H(B)_\rho$ is defined analogously,

$$H(A)_\rho + H(B)_\rho > -\log c. \quad (2)$$

c denotes the *maximum overlap* between any eigenstates, $|a\rangle$ and $|b\rangle$, of the observables' eigenstates: $c := \max_{a,b} \{|\langle b|a \rangle|^2\}$. Inequality (2) holds for every state ρ and eliminates state dependence from the bound (RHS), as desired.

The uncertainty relations (1) and (2) concern only projective, or strong, measurements of observables. *Weak measurements* [10] operate at various measurement strengths. They have been explored recently in quantum optics [11], cavity quantum electrodynamics (QED) [12], and circuit QED [13–16]. During a weak measurement, the system of interest is coupled weakly to a detector ancilla, which is then projected [17]. The outcome provides partial information about the system of interest, without projecting the system. Weak measurements illuminate quantum dynamics, as in the tracking of the progress of spontaneous emission [18, 19], the catching and reversing of quantum jumps [20], and observations of noncommuting observables' dynamics [21].

An entropic uncertainty relation that governs weak measurements was proved recently [22]. The relation quantifies the disagreement between a strong measurement and the composition of a weak measurement and another strong measurement. We show that the weak measurement can, backacting on the state, reconcile the disagreement between the strong measurements. The measurements are performed in a circuit-QED architecture, with a superconducting transmon qubit.

Our results reveal a physical significance of weak values. A *weak value* is a preselected and postselected expectation value. Let $\mathcal{I} = \sum_i \lambda_i |i\rangle\langle i|$ and $F = \sum_f f |f\rangle\langle f|$ denote observables. We assume, throughout this paper, that the eigenspaces are nondegenerate, as we will focus on a qubit. But this formalism, and the theory we test [22], extend to degeneracies. Consider measuring \mathcal{I} ,

obtaining outcome λ_i , measuring F , and obtaining outcome f . Let A denote an observable that commutes with neither \mathcal{I} nor F . Which value can be retrodictively ascribed most reasonably to A , given the preselection on λ_i and the postselection on f ? The weak value [23]

$$A_{\text{wv}} := \frac{\langle f | A | i \rangle}{\langle f | i \rangle}. \quad (3)$$

A_{wv} can assume anomalous values, which lie outside the operator's spectrum. Weak values significance and utility have been debated across theory and experiment [24? – 28].

We demonstrate a new physical meaning of the weak value: As a contribution to the uncertainty bound for weak and strong measurements [22], A_{wv} controls how much weak measurements reconcile incompatibility.

This paper reports on an experimental test of the entropic uncertainty relation for weak and strong measurements [22]. We first introduce the experimental platform and the dispersive measurements performed in circuit QED. We begin by quantifying two projective measurements' incompatibility with entropies. Turning one measurement into a composition—a weak measurement followed by a projective measurement—raises the overall measurement's entropy by increasing the number of possible outcomes. But, under a natural normalization scheme, the weak measurement reduces the sum of the two operations' entropies. The entropy sum was bounded in [22], whose theory we review and then test experimentally. We quantify how the weak measurement backacts on the state. Through the backaction, the weak value can lower the uncertainty bound, allowing the measurements to agree more.

Experimental context.—We measure the entropic uncertainty relation with a transmon superconducting qubit. The qubit couples to one mode of the electromagnetic field in a three-dimensional microwave cavity (Fig. 1). The qubit frequency, $\omega_q/(2\pi) = 3.889$ GHz, is far detuned from the cavity frequency, $\omega_c/(2\pi) = 5.635$ GHz, enabling a dispersive interaction. Dispersive interactions do not exchange energy, allowing for quantum-nondemolition measurements. The Jaynes-Cummings Hamiltonian in the dispersive limit,

$$H_{\text{JC}}/\hbar = \omega_c a^\dagger a + \frac{1}{2} \omega_q \sigma_z + \chi a^\dagger a \sigma_z, \quad (4)$$

governs the measurement dynamics. a^\dagger (a) denotes the cavity mode's creation (annihilation) operator, and σ_z denotes the Pauli z operator. The final term, $\chi a^\dagger a \sigma_z$, represents the interaction. It effectively changes ω_c by an amount $\pm \chi = \mp 2\pi(1.5 \text{ MHz})$ dependent on the qubit's state.

We prepare the cavity probe in a coherent state, whose phase shifts in accordance with the qubit's state. We perform a homodyne measurement of the field's Q quadrature, using a Josephson parametric amplifier. The probe

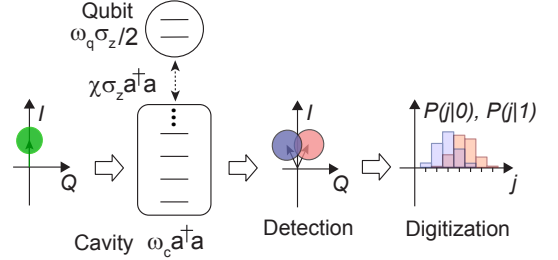


FIG. 1. Our experimental setup involves a superconducting transmon qubit coupled dispersively to a microwave cavity. The cavity's state is sketched in phase space, defined by quadratures I and Q . Coherent states probe the cavity, acquiring a phase shift (red and blue circles) dependent on the qubit's state. The transmitted-probe quadrature that contains qubit-state information is demodulated and digitized into discrete measurement outcomes j .

state is continuous-variable. However, we discretize the possible measurement outcomes into bins labeled by j .

Outcome j occurs with a probability calculated with a positive operator-valued measure (POVM). POVMs represent general (not-necessarily-projective) measurements mathematically [8]. A POVM is a set of positive operators $K_j^\dagger K_j > 0$ that obey the normalization condition $\sum_j K_j^\dagger K_j = I$. The *Kraus operator* K_j evolves the system-of-interest state: $\rho \mapsto K_j \rho K_j^\dagger / \text{Tr}(\rho K_j^\dagger K_j)$. The denominator equals the measurement's probability of yielding j .

Our setup measures the qubit observable $A = \sigma_z$, due to Eq. (4) and the measurement's homodyne nature. We can effectively measure other observables A by rapidly rotating the qubit before and after the interaction. If the homodyne measurement yields outcome j , the qubit state evolves under the Kraus operator [29, 30]

$$K_j = \left(\frac{\delta t}{2\pi\tau} \right)^{1/4} \exp \left(-\frac{\delta t}{4\tau} [jI - A]^2 \right). \quad (5)$$

τ denotes the characteristic measurement time [31], and the integration time δt determines the measurement strength $\delta t/\tau$. It depends on system parameters including the mean number of photons in the cavity. The Kraus operator's backaction on the qubit state will enable the weak measurement to reconcile incompatible operators.

Entropic uncertainties.—To build intuition, we show how entropic uncertainties arise in our experiment and are modified by weak measurements. First, we define observables \mathcal{I} , F , and A . Without loss of generality, we set $\mathcal{I} = \sigma_z = |0\rangle\langle 0| - |1\rangle\langle 1|$. F is represented on the Bloch sphere by the axis that lies an angle θ_F below the z -axis, at the azimuthal angle $\phi = 0$ [Fig. 2(a)]. A is defined analogously, in terms of θ_A .

Consider preparing a state ρ and implementing one of the three measurements shown in Fig. 2(a): (i) a projec-

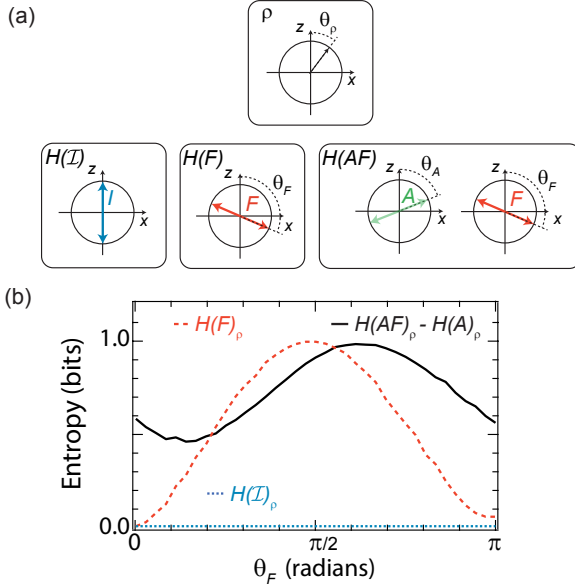


FIG. 2. Characterization of entropic uncertainties: (a) We subject a state ρ to one of three measurements. The measurements' entropies are defined as the detectors' von Neumann entropies. (b) Entropies measured for the state $\rho = |0\rangle\langle 0|$. $H(I)_\rho$ and $H(F)_\rho$ characterize projective measurements. $H(AF)_\rho - H(A)_\rho$ quantifies the change, caused by the weak measurement, in the second measurement's entropy, when $\theta_A = \pi/4$. $H(I)_\rho + H(F)_\rho$ maximizes when $\theta_F = \pi/2$, such that $F = X$, while $I = Z$. The second measurement's entropy change, $H(AF)_\rho - H(A)_\rho$, maximizes at $\theta_F = 0.53\pi$.

tive measurement of I , (ii) a projective measurement of F , or (iii) the composition of a weak A measurement and a subsequent projective F measurement. We implement a projective measurement experimentally by integrating the measurement signal for a time $\delta t \gg \tau$. Choosing $\delta t = 350$ ns and $\tau = 6$ ns realizes a projective measurement with ground-state-fidelity 99% and excited-state-fidelity 91%.

The entropies $H(I)_\rho$ and $H(F)_\rho$ are defined as follows. In each of many trials, we prepare a qubit state ρ and measure I . From the outcome statistics, we infer the probabilities $p_i = \langle i | \rho | i \rangle$. From $\{p_i\}$, we calculate $H(I)_\rho$. We determine $H(F)_\rho$ analogously. For the data shown in Fig. 2(b), $\rho = |0\rangle\langle 0|$. The entropies' sum peaks at $\theta_F = \pi/2$, signaling the maximal incompatibility of σ_z with $\pm \sigma_x$. I and F coincide at $\theta_F = 0$, where the entropy sum minimizes. The sum $\gtrsim 0$ because the measurements have finite fidelities.

Figure 2(b) displays also the entropy of the joint AF measurement, for $\theta_A = \pi/4$. In each of many trials, we prepare ρ , measure A weakly, and measure F projectively. From the frequencies of the outcome tuples (j, f) , we infer the joint probabilities $p_{j,f} = \langle f | K_j \rho K_j^\dagger | f \rangle$. On the distribution, we calculate the entropy $H(AF)_\rho$.

j assumes one of $\approx 2^4$ possible values, so the weak

measurement raises the entropy by ≈ 4 bits. Aside from this increase, measuring A reduces entropy sum when $\theta_F = \pi/2$, where $F = \sigma_x$ disagrees maximally with $I = \sigma_z$. To highlight this effect, we normalize $H(AF)_\rho$, displaying the difference $H(AF)_\rho - H(A)_\rho$ in Fig. 2(b). The weak A measurement reconciles the two operators, as we now quantify in more detail.

Theory.—We briefly review the derivation of the entropic uncertainty relation for weak and strong measurements [22]. For convenience, we reuse the definitions in the previous two sections. The theory generalizes, however, beyond circuit QED and qubits. Recall two of our POVMs, (i) a projective I measurement and (iii) the composition of a weak A measurement and a projective F measurement.

We formalize a general weak measurement as follows. A detector is prepared in a state $|D\rangle$, coupled to the system's A weakly via a unitary V , and measured projectively. If outcome j obtains, the system evolves under the Kraus operator $K_j = (\text{phase}) \langle j | V | D \rangle$. Taylor-approximating in the coupling strength yields [32]

$$K_j = \sqrt{p_j} \{ I + g_j A + O([g_j]^2) \}. \quad (6)$$

p_j equals the probability that, if the detector is prepared in $|D\rangle$ and does not couple, the measurement yields j . g_j quantifies the interaction strength and is defined, via the Kraus operators' unitary invariance [8], to be real. Comparing with Eq. (5), we calculate the cavity-QED p_j and g_j in the Supplemental Material [33].

The entropic uncertainty relation for weak and strong measurements is proved as follows. We begin with a generalization, to POVMs, of the entropic uncertainty relation (2) [34, 35]. POVMs (i) and (iii) are substituted into the relation. The left-hand side (LHS), $H(I)_\rho + H(AF)_\rho$, consists of entropies defined as in the previous section. The entropies quantify the average uncertainties about the POVMs' outcomes.

The uncertainty relation's RHS contains a maximum overlap, similarly to Ineq. (2). This overlap, however, is between POVM elements. In its raw form, the RHS cannot be straightforwardly inferred from experiments. Therefore, the bound was Taylor-approximated in the weak coupling, $g_j \sqrt{p_j}$. The entropic uncertainty relation for strong and weak measurements results:

$$H(I)_\rho + H(AF)_\rho \geq \min_{i,j,f} \left\{ -\log_2(p_{f|i} p_j) - \frac{2}{\ln 2} \Re(g_j A_{\text{wv}}) + O(p_j [g_j]^2) \right\}. \quad (7)$$

The bound contains two non-negligible terms. The zeroth-order term depends on the eigenstate overlap $p_{f|i} = |\langle f | i \rangle|^2$ in the entropic uncertainty relation (2) for projective measurements. The first-order-term depends on the weak value, A_{wv} [Eq. (3)]. Positive weak values tend to achieve the minimum, we find, leading to a negative A_{wv} term. The term lowers the bound, enabling the POVMs to agree more, as our experiment shows.

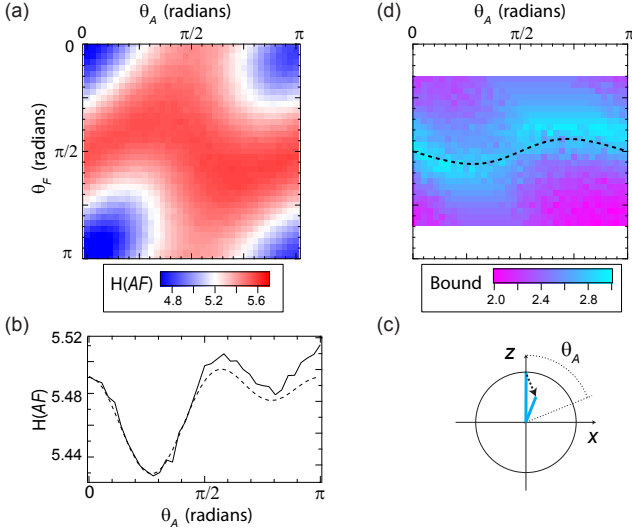


FIG. 3. Measurements of the entropic uncertainty relation: (a) the entropy $H(AF)_\rho$ and (d) the bound. The dashed line indicates the bound's theoretical maximum. (b) Detail of $H(AF)_\rho$ versus θ_A , compared to theory (dashed line), at $\theta_F = \pi/2$. (c) Bloch-plane sketch indicating the A measurement's backaction (dashed arrow) on the initial state.

Results.—Figure 3 displays results of measuring both sides of the entropic uncertainty relation (7). As above, we set $\mathcal{I} = \sigma_z$ and $\rho = |0\rangle\langle 0|$, to achieve the tightest bound. Since the \mathcal{I} -measurement axis coincides with ρ on the Bloch sphere, only the measurement infidelity causes the entropy $H(\mathcal{I})_\rho$ (Fig. 2) to contribute to the LHS of (7). We first focus on $H(AF)_\rho$, measured as a function of θ_F and θ_A . The choice $\mathcal{I} = \sigma_z$ introduces an azimuthal symmetry that allows us to neglect rotations out of the x - z plane.

We have already detailed the θ_F -dependence of $H(AF)_\rho$ for $\theta_A = \pi/4$: Figure 2 showed how the weak measurement can reconcile incompatible operators. Here, we focus on the θ_A dependence of $H(AF)_\rho$ [Fig. 3(b)]. Four effects compete to extremize $H(AF)_\rho$ as a function of $\theta_A \in [0, \pi]$, when $\theta_F = \pi/2$. First, as θ_A grows from 0, the initial states overlap with an A eigenstate decreases. A -measurement outcomes are sampled from an increasingly uniform distribution. This effect helps maximize $H(AF)_\rho$ at $\theta_A = \pi/2$. Second, as A approaches F , the A measurement's backaction biases the F -measurement outcome. This effect would decrease $H(AF)_\rho$ to a minimum at $\theta_A = \pi/2$, in the absence of the other effects. Third, the weak measurement partially projects the state onto the A axis, dephasing the state with respect to the A eigenbasis. Detection inefficiency enhances the dephasing [33] and shrinks the Bloch vector [Fig. 3(c)]. The F -measurement outcome becomes maximally biased, minimizing $H(AF)_\rho$, when $\theta_A = \pi/4, 3\pi/4$. Fourth, readout infidelity (due to energy leakage from the

qubit) raises $H(AF)_\rho$ as θ_A increases. Hence $H(AF)_\rho$ is asymmetric about $\theta_A = \pi/2$. Overall, the maxima and minima of $H(AF)$ follow from the competition between the uncertainties in the F -measurement and A -measurement outcomes. Our experimental apparatus's finite measurement efficiency [33] masks the A measurements contribution, resulting in minima at $\theta_A = \pi/4$ and $3\pi/4$.

Figure 3(d) displays measured values of the entropic uncertainty relation's RHS. We measure $p_{f|i}$, p_j , and A_{wv} in separate sets of experiments. We calculate $p_{f|i} = |\langle f|i \rangle|^2$ by preparing an \mathcal{I} eigenstate $|i\rangle$ and measuring F in each of many trials. From the frequency with which f occurs, we infer the conditional probability. The p_j and g_j in (6) are obtained from the weak-measurement calibration [33]. Finally, we measure the weak value A_{wv} by preparing an \mathcal{I} eigenstate $|i\rangle$, measuring A weakly, and then measuring F projectively, in each of many trials. Then, we postselect on the final-measurement outcome f . An average of the weak-measurement outcomes j is proportional to A_{wv} [33]. We measure the uncertainty relation's RHS only where $\theta_F \in [\pi/6, 5\pi/6]$, due to low postselection-success rates closer to 0 and to π . Having measured $p_{f|i}$, p_j , and A_{wv} for each choice of (i, j, f) , we calculate the argument of the minimum in Ineq. (7). We then identify the minimizing triple.

In Fig. 3(d), the maximum of the bound, the inequality's RHS, varies sinusoidally with θ_A . Though F disagrees most with \mathcal{I} at $\theta_F = \pi/2$, the weak A measurement shifts the maximum's location. For example, when $\theta_A = \pi/4$, the maximally disagreeing AF measurement has $\theta_F = 0.53\pi$, when the measurement strength is $\delta t/\tau = 0.17$. When $\theta_F = \pi/2$, setting θ_A to $\pi/4$ reconciles disagreeing operators, σ_z and σ_x .

The weak value [Eq. (3)] underlies the reconciliation. The weak-value term in Ineq. (7) tends to assume negative values, lowering the bound. Weak values A_{wv} can grow anomalous, straying outside the A spectrum. However, large A_{wv} values can violate the Taylor approximation that led to Ineq. (7) [22], so they are irrelevant to our uncertainty relation.

Finally, we examine the bound's tightness, the difference between the LHS and RHS. The bound tightens maximally not just at one measurement orientation, but across a set of orientations near $\theta_F = \pi/2$. Here, the tightness is 2.45 ± 0.05 bits. Inefficient detection accounts for 1.66 of the bits.

Discussion.—We have experimentally measured an entropic uncertainty relation for strong and weak measurements [22], using a circuit-QED platform. A weak measurement, we have shown, can reconcile incompatible operations: up to a normalization floor, the weak measurement decreases the entropy sum on the inequality's LHS and the uncertainty bound on the RHS. This work opens operator reconciliation to feedback-free control by weak measurements, which have recently been used to con-

trol steering [36] and pure-state preparation [37] without feedback. This work also suggests benefits of using weak measurements in applications of entropic uncertainty relations, as to quantum cryptography [38].

Mathematically, a weak value lowers the uncertainty relation's RHS. The weak value's influence is visible also in the sinusoidal variation of the RHS with the weak-measurement angle. This work therefore demonstrates a new physical interpretation of the weak value: the weak value controls the uncertainty bound on operations formed from strong and weak measurements. Whereas other interpretations have excited controversy, this interpretation is, we believe, mathematically clear and experimentally supported.

Entropic uncertainty relations have been measured with various platforms, including neutrons, optics, and nitrogen-vacancy centers [39–42]. The measurements in [42], though nonprojective, are probabilistic projections. In contrast, our measurements are weak and experimentally demonstrate the weak value's role in reconciling incompatible operations. This role has only been mentioned theoretically [22], neither detailed nor experimentally tested, until now. Uncertainty relations occupy two categories [7], one centered on measurement outcomes' unpredictability [41, 42] and one centered on measurements' disturbance of quantum states [39, 40]. Our uncertainty relation occupies both categories, in the spirit of [43]: on the one hand, we prepare an \mathcal{I} eigenstate $|i\rangle$ and perform the composite AF measurement. On the other hand, we take advantage of the weak A measurement's disturbance of $|i\rangle$. This work identifies weak measurements as a means of unifying the classes of uncertainty relations.

The measured uncertainty relation follows from simplifying an entropic uncertainty relation for quantum information scrambling [22]. Quantum information *scrambles* by spreading through many-body entanglement, during a nonclassical stage of equilibration [44–47]. The entropic uncertainty relation for quantum-information scrambling occupies a recent line of theoretical applications of weak measurements to scrambling [22, 48–54]. Our experiment is the first to arise from this theory. It paves the way for characterizations of scrambling with weak measurements of many-body quantum systems.

Acknowledgments—KWM acknowledges support from NSF No. PHY- 1752844 (CAREER) and use of facilities at the Institute of Materials Science and Engineering at Washington University. NYH is grateful for funding from the Institute for Quantum Information and Matter, an NSF Physics Frontiers Center (NSF Grant PHY-1125565) with support of the Gordon and Betty Moore Foundation (GBMF-2644), and for an NSF grant for the Institute for Theoretical Atomic, Molecular, and Optical Physics at Harvard University and the Smithsonian Astrophysical Observatory. This project began at the KITP's 2018 “Quantum Thermodynamics” conference

and so was supported in part by the National Science Foundation under Grant No. NSF PHY-1748958.

REFERENCES

- * j.monroe@wustl.edu
- † nicoleyh@g.harvard.edu
- ‡ murch@physics.wustl.edu
- [1] J. E. A. Aasi, Enhanced sensitivity of the LIGO gravitational wave detector by using squeezed states of light, *Nature Photonics* **7**, 613 (2013).
- [2] C. L. Degen, F. Reinhard, and P. Cappellaro, Quantum sensing, *Reviews of Modern Physics* **89**, 1 (2017).
- [3] C. M. Caves, Quantum limits on noise in linear amplifiers, *Physical Review D* **26**, 1817 (1982).
- [4] A. A. Clerk, M. H. Devoret, S. M. Girvin, F. Marquardt, and R. J. Schoelkopf, Introduction to quantum noise, measurement, and amplification, *Reviews of Modern Physics* **82**, 1155 (2010), arXiv:0810.4729.
- [5] H. P. Robertson, The Uncertainty Principle, *Physical Review* **34**, 163 (1929).
- [6] D. Deutsch, Uncertainty in quantum measurements, *Phys. Rev. Lett.* **50**, 631 (1983).
- [7] P. J. Coles, M. Berta, M. Tomamichel, and S. Wehner, Entropic uncertainty relations and their applications, *Reviews of Modern Physics* **89**, 10.1103/RevModPhys.89.015002 (2017).
- [8] M. A. Nielsen and I. L. Chuang, *Quantum computation and quantum information* (Cambridge University Press, Cambridge New York, 2000).
- [9] H. Maassen and J. B. M. Uffink, Generalized entropic uncertainty relations, *Physical Review Letters* **60**, 1103 (1988).
- [10] K. Jacobs and D. A. Steck, A straightforward introduction to continuous quantum measurement, *Contemporary Physics* **47**, 279 (2006), arXiv:0611067 [quant-ph].
- [11] S. Kocsis, B. Braverman, S. Ravets, M. J. Stevens, R. P. Mirin, L. K. Shalm, and A. M. Steinberg, Observing the average trajectories of single photons in a two-slit interferometer, *Science* **332**, 1170 (2011), <https://science.sciencemag.org/content/332/6034/1170.full.pdf>.
- [12] C. Guerlin, J. Bernu, S. Deléglise, C. Sayrin, S. Gleyzes, S. Kuhr, M. Brune, J.-M. Raimond, and S. Haroche, Progressive field-state collapse and quantum non-demolition photon counting, *Nature* **448**, 889 (2007).
- [13] R. Vijay, D. H. Slichter, and I. Siddiqi, Observation of quantum jumps in a superconducting artificial atom, *Physical Review Letters* **106**, 1 (2011).
- [14] M. Hatridge, S. Shankar, M. Mirrahimi, F. Schackert, K. Geerlings, T. Brecht, K. M. Sliwa, B. Abdo, L. Frunzio, S. M. Girvin, R. J. Schoelkopf, and M. H. Devoret, Quantum back-action of an individual variable-strength measurement, *Science* **339**, 178 (2013).
- [15] K. W. Murch, S. J. Weber, C. Macklin, and I. Siddiqi, Observing single quantum trajectories of a superconducting quantum bit, *Nature* **502**, 211 (2013), arXiv:1305.7270.
- [16] J. P. Groen, D. Ristè, L. Tornberg, J. Cramer, P. C. de Groot, T. Picot, G. Johansson, and L. DiCarlo, Partial-measurement backaction and nonclassical weak values in a superconducting circuit, *Phys. Rev. Lett.* **111**, 090506 (2013).

[17] J. Von Neumann, *Mathematische Grundlagen der Quantenmechanik*, Die Grundlehren der mathematischen Wissenschaften in Einzeldarstellungen (J. Springer, 1932).

[18] M. Naghiloo, N. Foroozani, D. Tan, A. Jadbabaie, and K. W. Murch, Mapping quantum state dynamics in spontaneous emission, *Nature Communications* **7**, 11527 (2016), arXiv:1512.02307.

[19] P. Campagne-Ibarcq, P. Six, L. Bretheau, A. Sarlette, M. Mirrahimi, P. Rouchon, and B. Huard, Observing Quantum State Diffusion by Heterodyne Detection of Fluorescence, *Physical Review X* **6**, 011002 (2016), arXiv:1511.01415.

[20] Z. K. Minev, S. O. Mundhada, S. Shankar, P. Reinhold, R. Gutiérrez-Jáuregui, R. J. Schoelkopf, M. Mirrahimi, H. J. Carmichael, and M. H. Devoret, To catch and reverse a quantum jump mid-flight, *Nature* **570**, 200 (2019), arXiv:1803.00545.

[21] S. Hacohen-Gourgy, L. S. Martin, E. Flurin, V. V. Ramalesh, K. B. Whaley, and I. Siddiqi, Quantum dynamics of simultaneously measured non-commuting observables, *Nature* **538**, 491 (2016), arXiv:1608.06652.

[22] N. Yunger Halpern, A. Bartolotta, and J. Pollack, Entropic uncertainty relations for quantum information scrambling, *Communications Physics* **2**, 92 (2019).

[23] Y. Aharonov, D. Z. Albert, and L. Vaidman, How the result of a measurement of a component of the spin of a spin- 1/2 particle can turn out to be 100, *Physical Review Letters* **60**, 1351 (1988).

[24] A. J. Leggett, Comment on How the result of a measurement of a component of the spin of a spin-(1/2 particle can turn out to be 100", *Physical Review Letters* **62**, 2325 (1989).

[25] Y. Aharonov, J. Anandan, S. Popescu, and L. Vaidman, Superpositions of time evolutions of a quantum system and a quantum time-translation machine, *Physical Review Letters* **64**, 2965 (1990).

[26] J. Dressel, M. Malik, F. M. Miatto, A. N. Jordan, and R. W. Boyd, Colloquium: Understanding quantum weak values: Basics and applications, *Reviews of Modern Physics* **86**, 307 (2014).

[27] O. Hosten and P. Kwiat, Observation of the Spin Hall Effect of Light via Weak Measurements, *Science* **319**, 787 (2008).

[28] A. N. Jordan, J. Martínez-Rincón, and J. C. Howell, Technical advantages for weak-value amplification: When less is more, *Phys. Rev. X* **4**, 011031 (2014).

[29] M. Boissonneault, J. M. Gambetta, and A. Blais, Dispersive regime of circuit qed: Photon-dependent qubit dephasing and relaxation rates, *Phys. Rev. A* **79**, 013819 (2009).

[30] M. Hatridge, S. Shankar, M. Mirrahimi, F. Schackert, K. Geerlings, T. Brecht, K. M. Sliwa, B. Abdo, L. Frunzio, S. M. Girvin, R. J. Schoelkopf, and M. H. Devoret, Quantum back-action of an individual variable-strength measurement, *Science* **339**, 178 (2013), <https://science.sciencemag.org/content/339/6116/178.full.pdf>.

[31] S. J. Weber, A. Chantasri, J. Dressel, A. N. Jordan, K. W. Murch, and I. Siddiqi, Mapping the optimal route between two quantum states, *Nature* **511**, 570 (2014).

[32] Our g_j is defined as the $g_j/\sqrt{p_j}$ in [22].

[33] See Supplemental Material.

[34] M. Tomamichel, *A Framework for Non-Asymptotic Quantum Information Theory*, Ph.D. thesis, ETH Zürich (2012).

[35] M. Krishna and K. Parthasarathy, An Entropic Uncertainty Principle for Quantum Measurements, eprint arXiv:quant-ph/0110025 (2001), quant-ph/0110025.

[36] S. Roy, J. T. Chalker, I. V. Gornyi, and Y. Gefen, Measurement-induced steering of quantum systems, arXiv e-prints , arXiv:1912.04292 (2019), arXiv:1912.04292 [cond-mat.stat-mech].

[37] J. T. Muhonen, J. P. Dehollain, A. Laucht, S. Simmons, R. Kalra, F. E. Hudson, A. S. Dzurak, A. Morello, D. N. Jamieson, J. C. McCallum, and K. M. Itoh, Coherent control via weak measurements in ^{31}P single-atom electron and nuclear spin qubits, *Phys. Rev. B* **98**, 155201 (2018).

[38] P. J. Coles and M. Piani, Complementary sequential measurements generate entanglement, *Physical Review A - Atomic, Molecular, and Optical Physics* **89**, 1 (2014).

[39] C. F. Li, J. S. Xu, X. Y. Xu, K. Li, and G. C. Guo, Experimental investigation of the entanglement-assisted entropic uncertainty principle, *Nature Physics* **7**, 752 (2011).

[40] R. Prevedel, D. R. Hamel, R. Colbeck, K. Fisher, and K. J. Resch, Experimental investigation of the uncertainty principle in the presence of quantum memory and its application to witnessing entanglement, *Nature Physics* **7**, 757 (2011).

[41] J. Xing, Y. R. Zhang, S. Liu, Y. C. Chang, J. D. Yue, H. Fan, and X. Y. Pan, Experimental investigation of quantum entropic uncertainty relations for multiple measurements in pure diamond, *Scientific Reports* **7**, 1 (2017).

[42] B. Demirel, S. Sponar, A. A. Abbott, C. Branciard, and Y. Hasegawa, Experimental test of an entropic measurement uncertainty relation for arbitrary qubit observables, *New Journal of Physics* **21**, 013038 (2019), arXiv:1711.05023.

[43] L. A. Rozema, A. Darabi, D. H. Mahler, A. Hayat, Y. Soudagar, and A. M. Steinberg, Violation of heisenberg's measurement-disturbance relationship by weak measurements, *Phys. Rev. Lett.* **109**, 100404 (2012).

[44] S. H. Shenker and D. Stanford, Black holes and the butterfly effect, *Journal of High Energy Physics* **3**, 67 (2014).

[45] D. A. Roberts and D. Stanford, Diagnosing Chaos Using Four-Point Functions in Two-Dimensional Conformal Field Theory, *Physical Review Letters* **115**, 131603 (2015).

[46] J. Maldacena, S. H. Shenker, and D. Stanford, A bound on chaos, ArXiv e-prints (2015), arXiv:1503.01409 [hep-th].

[47] A. Kitaev, A simple model of quantum holography (2015).

[48] N. Yunger Halpern, Jarzynski-like equality for the out-of-time-ordered correlator, *Physical Review A* **95**, 1 (2017).

[49] N. Yunger Halpern, B. Swingle, and J. Dressel, Quasiprobability behind the out-of-time-ordered correlator, *Phys. Rev. A* **97**, 042105 (2018).

[50] B. Swingle and N. Yunger Halpern, Resilience of scrambling measurements, *Phys. Rev. A* **97**, 062113 (2018).

[51] J. R. González Alonso, N. Yunger Halpern, and J. Dressel, Out-of-time-ordered-correlator quasiprobabilities robustly witness scrambling, *Phys. Rev. Lett.* **122**, 040404 (2019).

[52] J. Dressel, J. R. González Alonso, M. Waegell, and N. Yunger Halpern, Strengthening weak measurements of qubit out-of-time-order correlators, *Phys. Rev. A* **98**,

012132 (2018).

[53] R. Mohseninia, J. R. G. Alonso, and J. Dressel, Optimizing measurement strengths for qubit quasiprobabilities behind out-of-time-ordered correlators, *Phys. Rev. A* **100**, 062336 (2019).

[54] D. R. M. Arvidsson-Shukur, N. Yunger Halpern, H. V. Lepage, A. A. Lasek, C. H. W. Barnes, and S. Lloyd, Quantum advantage in postselected metrology, *Nature Communications* **11**, 3775 (2020).

[55] In the main text, we denoted joint and conditional probabilities by $p_{j,f}$ and $p_{f|i}$. The number of joint and conditional probabilities will grow in this Supplementary Material. For ease of reading, therefore, we change the notation to $p(j,f)$, $p(f|i)$, etc.

Supplemental Material

EXPERIMENTAL SETUP

The experimental setup consists of a superconducting transmon circuit embedded in a three-dimensional copper cavity. The cavity is shielded in a copper enclosure and encased in aluminum and Cryoperm magnetic shields. The cavity is coupled to a $50\ \Omega$ transmission line that is directed, via a microwave circulator, to a Josephson parametric amplifier. The amplifier operates with ~ 10 MHz of instantaneous bandwidth in phase-sensitive mode. The microwave setup is similar to that in Ref. [15]. The transmon and amplifier were fabricated with direct-write photolithography and double-angle evaporation of aluminum on an intrinsic silicon wafer.

CALIBRATION MEASUREMENTS

To calibrate the measurement strength, we probe the cavity, near resonance, with a microwave drive. We examine the ensemble dephasing rate and the ac Stark shift, which are related to system parameters as $\Gamma_m = 8\chi^2\bar{n}/\kappa$ and $2\chi\bar{n}$, respectively. The cavity linewidth, measured in transmission through the cavity with a vector network analyzer, is $\kappa/(2\pi) = 4.5$ MHz. From these values, we infer the dispersive coupling rate, $\chi/(2\pi) = -1.5$ MHz, and the mean intracavity photon number, $\bar{n} = 0.5$.

The quantum efficiency reduces the signal-to-noise ratio with which we resolve the quantum states. We treat the quantum efficiency as noise added to our measurement signal. To calibrate the quantum efficiency, we prepare the qubit in the state $\rho_0 = |0\rangle\langle 0|$, then measure $A = \sigma_z$ weakly, in each of many trials. In another set of trials, $\rho = |1\rangle\langle 1|$. The probability of obtaining outcome j follows from introducing the quantum efficiency η into the Kraus operator (5):

$$p_{j|\rho} = \text{Tr}(\rho K_j^\dagger K_j) = \left(\frac{\delta t \eta}{2\pi\tau} \right)^{1/2} \exp \left(-\frac{\delta t \eta}{2\tau} [j \pm 1]^2 \right),$$

with ρ_0 corresponding to $\pm = +$ and ρ_1 corresponding to $\pm = -$. We have introduced the ensemble characteristic measurement time $\tau = 1/(2\Gamma_m) = \kappa/(16\chi^2\bar{n})$.

In the experiment, we measure only σ_z directly. To measure different observables, we rotate the state before and after the σ_z measurement.

MINIMA OF $H(AF)$

In the main text, we discussed the extrema of $H(AF)_\rho$ as functions of $\theta_A \in [0, \pi]$, with $\theta_F = \pi/2$ and $\rho = |0\rangle\langle 0|$. We observed that ensemble-level dephasing, induced by the weak A measurement, biases the F -measurement outcome. As a result, $H(AF)_\rho$ minimizes at $\theta_A = \pi/4$ and $3\pi/4$. Surprisingly, a direct calculation of $H(AF)_\rho$ exhibits *maxima* at $\theta_A = \pi/4$ and $3\pi/4$. The seeming contradiction arises because the changes in the joint distribution over (j,f) outcomes are small. Inefficient detection masks the small changes. Hence ensemble-level evolution dominates the qualitative behavior of $H(AF)_\rho$.

Our measurements agree fairly well with a model that includes inefficient detection. We model inefficient detection via a two-measurement process [10]. One measurement record describes the detected outcome, and the other measurement record describes an outcome lost to the environment. Averaging over all possible values of the lost outcome increases the detected outcome's variance.

HOW THE WEAK VALUE IS MEASURED

Our measurement strategy relies on a proportionality proved in the next section: The real part of the weak value, $\Re(A_{\text{wv}})$, is proportional to the average preselected and postselected detector outcome, $\langle\langle j \rangle\rangle$. To measure $\langle\langle j \rangle\rangle$, we prepare a state ρ_0 , rotate it downward toward the x -axis through an angle $-\theta_A$, measure σ_z weakly for 250 ns, and rotate the state back. This measurement process yields an outcome j . Finally, we measure the observable F projectively, obtaining an outcome f . We repeat this protocol in many trials. Processing the outcome statistics, as dictated in the next section, yields $\langle\langle j \rangle\rangle$.

PROPORTIONALITY BETWEEN THE WEAK VALUE A_{wv} AND AN AVERAGE OF j

Consider preparing a system of interest in a state $|i\rangle$, coupling the detector to a system observable $A = \sum_a a|a\rangle\langle a|$, measuring the detector strongly, and then measuring a system-of-interest observable $F = \sum_f f|f\rangle\langle f|$ strongly. Let f denote the F measurement's outcome. The measurement of the detector yields a random variable j . An average of j is proportional to the weak value A_{wv} . We define the average and derive the proportionality constant here.

We choose for our model to have two features that merit explaining. First, we assume that the system of interest is a qubit, as in the main text. A represents a Pauli operator, which squares to the identity operator: $A^2 = I$. Second, j is continuous ideally, and we model it as continuous, here, for convenience. In an experiment, however, j values are binned, so the variable is discretized.

The probability of obtaining outcome f , conditioned on one's having prepared i and obtained j , equals [55]

$$p(f|i, j) = |\langle f | K_j | i \rangle|^2 \quad (\text{S1})$$

$$= p_j \left\{ p(f|i) + 2\Re(g_j \langle i | f \rangle \langle f | A | i \rangle) + O([g_j]^2) \right\}. \quad (\text{S2})$$

We have substituted in for K_j from Eq. (6). $p(f|i) = |\langle f | i \rangle|^2$ denotes the conditional probability that preparing $|i\rangle$ and measuring F yields f . The $\langle f | A | i \rangle$ equals the numerator in the definition of A_{wv} [Eq. (3)]. We substitute $\langle f | i \rangle A_{\text{wv}}$ into Eq. (S2). Dividing each side of the equation by $p(f|i)$ simplifies the RHS:

$$\frac{p(f|i, j)}{p(f|i)} = p_j \left\{ 1 + 2\Re(g_j A_{\text{wv}}) + O([g_j]^2) \right\}. \quad (\text{S3})$$

Bayes' theorem offers an interpretation of the LHS of Eq. (S3). We derive the interpretation by writing two expressions for the joint probability $p(i, j, f)$ of preparing $|i\rangle$, then obtaining j and f ,

$$\begin{aligned} p(i, j, f) &= p(f|i, j) p(i, j) = p(f|i, j) p(j|i) p(i) \\ &= p(f|i, j) p(j|i) \quad \text{and} \end{aligned} \quad (\text{S4})$$

$$\begin{aligned} p(i, j, f) &= p(j|i, f) p(i, f) = p(j|i, f) p(f|i) p(i) \\ &= p(j|i, f) p(f|i). \end{aligned} \quad (\text{S5})$$

$p(i) = 1$ because our protocol requires a deterministic preparation of $|i\rangle$. We equate (S4) and (S5), then solve for the LHS of Eq. (S3):

$$\frac{p(f|i, j)}{p(f|i)} = \frac{p(j|i, f)}{p(j|i)}. \quad (\text{S6})$$

This ratio reflects the impact of the f —of the postselection—on the probability.

We simplify the calculation of the RHS of Eq. (S3), by stipulating that the detector be calibrated as follows. Suppose that the detector is prepared, is not coupled to the system of interest, and is measured strongly. The average outcome j is set to zero: $\int dj \cdot j \cdot p_j = 0$. This calibration condition amounts to a choice of a plot's origin. We invoke this condition upon integrating j against the RHS of Eq. (S3):

$$\langle\langle j \rangle\rangle := \int_{-\infty}^{\infty} dj \cdot j \frac{p(j|i, f)}{p(j|i)} \quad (\text{S7})$$

$$= \int_{-\infty}^{\infty} dj \cdot j p_j \left\{ 2\Re(g_j A_{\text{wv}}) + O([g_j]^2) \right\}. \quad (\text{S8})$$

We simplify and decompose the integral by specializing to our weak-measurement setup. The outcome-dependent coupling g_j is real, so $\Re(g_j A_{\text{wv}}) = g_j \Re(A_{\text{wv}})$. We calculate p_j and g_j by Taylor-approximating the RHS of Eq. (5) and comparing the result with Eq. (6):

$$\sqrt{p_j} = \left(\frac{\delta t}{2\pi\tau} \right)^{1/4} \exp \left(-\frac{\delta t}{4\tau} [j^2 + 1] \right), \quad \text{and} \quad (\text{S9})$$

$$g_j = \frac{\delta t}{2\tau} j. \quad (\text{S10})$$

We substitute from these equations into Eq. (S8) and evaluate the integral.

In our experiment, $g_j \leq 0.3$, and $|A_{\text{wv}}| \approx 1$. Hence the $O([g_j]^2)$ term in Eq. (S8) is about an order of magnitude less than the first term, and

$$\boxed{\langle \langle j \rangle \rangle \approx \Re(A_{\text{wv}}) e^{-\delta t/(2\tau)}}. \quad (\text{S11})$$

Since the coupling is weak, $\frac{\delta t}{\tau} \ll 1$, $e^{-\delta t/(2\tau)} \approx 1$, and $\langle \langle j \rangle \rangle \approx \Re(A_{\text{wv}})$.